ARMY RESEARCH LABORATORY

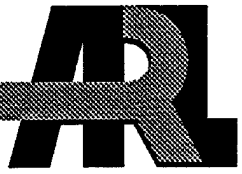

A Ballistic Evaluation of Ti-6A1-4V vs. Long Rod Penetrators

Matthew S. Burkins
U.S. ARMY RESEARCH LABORATORY

Jack I. Paige
Jeffrey S. Hansen
U.S. BUREAU OF MINES

ARL-TR-1146 July 1996

DISCLAIMER NOTICE

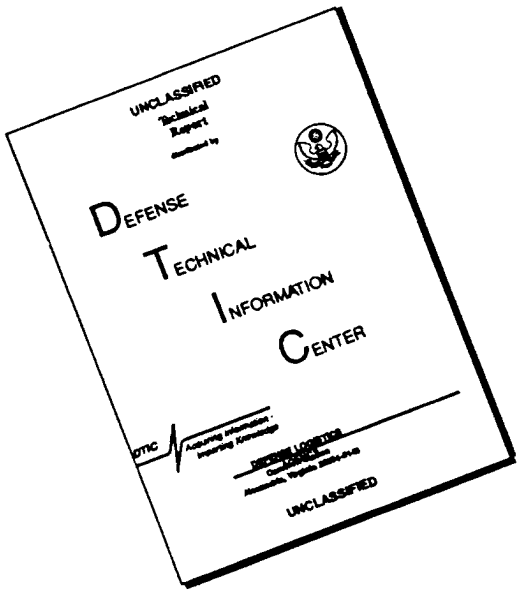

THIS DOCUMENT IS BEST QUALITY AVAILABLE. THE COPY FURNISHED TO DTIC CONTAINED A SIGNIFICANT NUMBER OF PAGES WHICH DO NOT REPRODUCE LEGIBLY.

NOTICES

Destroy this report when it is no longer needed. DO NOT return it to the originator.

Additional copies of this report may be obtained from the National Technical Information Service, U.S. Department of Commerce, 5285 Port Royal Road, Springfield, VA 22161.

The findings of this report are not to be construed as an official Department of the Army position, unless so designated by other authorized documents.

The use of trade names or manufacturers' names in this report does not constitute indorsement of any commercial product.

REPORT DOCUMENTATION PAGE

Form Approved
OMB No. 0704-0188

1. AGENCY USE ONLY *(Leave blank)*	2. REPORT DATE	3. REPORT TYPE AND DATES COVERED
	July 1996	Final, 1990 - 1992

4. TITLE AND SUBTITLE

A Ballistic Evaluation of Ti-6A1-4V vs. Long Rod Penetrators

5. FUNDING NUMBERS

PR: 622601DC05

6. AUTHOR(S)

Matthew S. Burkins, Jack I. Paige,* and Jeffrey S. Hansen*

7. PERFORMING ORGANIZATION NAME(S) AND ADDRESS(ES)

U.S. Army Research Laboratory
ATTN: AMSRL-WT-TA
Aberdeen Proving Ground, MD 21005-5066

8. PERFORMING ORGANIZATION REPORT NUMBER

ARL-TR-1146

9. SPONSORING/MONITORING AGENCY NAMES(S) AND ADDRESS(ES)

10.SPONSORING/MONITORING AGENCY REPORT NUMBER

11. SUPPLEMENTARY NOTES

*U.S. Bureau of Mines

12a. DISTRIBUTION/AVAILABILITY STATEMENT

Approved for public release; distribution is unlimited.

12b. DISTRIBUTION CODE

13. ABSTRACT *(Maximum 200 words)*

Previous research by the U.S. Army Materials Technology Laboratory, Watertown, MA, has shown that the most common titanium alloy, Ti-6Al-4V, provides weight-effective protection against small arms projectiles. Little follow-on research was performed with larger projectiles because the high cost of titanium precluded its use in land vehicle applications. However, since the cost of titanium has fallen relative to the cost of composite and ceramic armors, titanium is now a valid option for many armor applications calling for a lighter, nonmagnetic, noncorroding alternative for steel.

However, before titanium could be considered for such applications, baseline ballistic performance information against modern tungsten alloy (WA) and depleted uranium (DU) alloy penetrators was required. A joint test program between the U.S. Army Research Laboratory, Aberdeen Proving Ground, MD, and the U.S. Bureau of Mines, Albany, OR, was conducted to determine this necessary information about Ti-6Al-4V alloy. Baseline penetration and perforation data for Ti-6A1-4V and for standard rolled homogeneous armor (RHA) steel (MIL-A-12560) were collected. Ti-6A1-4V alloy showed a significant ballistic performance improvement over conventional RHA steel for both WA and DU penetrators. This report summarizes information presented at the ASM International Aeromat '94 Conference in Anaheim, CA, in June 1994.

14. SUBJECT TERMS	15. NUMBER OF PAGES
titanium, depleted uranium, tungsten, armor	46
	16. PRICE CODE

17. SECURITY CLASSIFICATION OF REPORT	18. SECURITY CLASSIFICATION OF THIS PAGE	19. SECURITY CLASSIFICATION OF ABSTRACT	20. LIMITATION OF ABSTRACT
UNCLASSIFIED	UNCLASSIFIED	UNCLASSIFIED	UL

INTENTIONALLY LEFT BLANK.

TABLE OF CONTENTS

		Page
	LIST OF FIGURES	v
	LIST OF TABLES	vii
1.	INTRODUCTION	1
2.	BACKGROUND	2
3.	TEST METHODOLOGY	3
4.	TEST PENETRATORS	6
5.	RESULTS	9
6.	CONCLUSIONS	15
7.	REFERENCES	17
	APPENDIX A: MATERIAL PROPERTY DATA FOR Ti-6A1-4V PLATES	19
	APPENDIX B: DETAILED FIRING DATA FOR Ti-6A1-4V AND RHA	33
	DISTRIBUTION LIST	41

INTENTIONALLY LEFT BLANK.

LIST OF FIGURES

Figure		Page
1.	Schematic of test setup	5
2.	Model scale penetrators	7
3.	Photograph of sectioned impact crater of tungsten penetrator into annealed T-6A1-4V plate (shot no. 2640)	11
4.	Penetration and perforation results for L/D = 10 X21	12
5.	Penetration and perforation results for L/D = 10 DU	13
6.	Photograph of typical exit hole in RHA	14
7.	Photograph of typical exit spall in annealed Ti-6A1-4V	14
8.	Photograph of typical exit spall in STA Ti-6A1-4V	15
A-1.	Photomicrographs for BOM plate no. 102	24
A-2.	Photomicrographs for BOM plate no. 104	25
A-3.	Photomicrographs for BOM plate no. 115	26
A-4.	Photomicrographs for BOM plate no. 116	27
A-5.	Photomicrographs for BOM plate no. 117	28
A-6.	Photomicrographs for BOM plate no. 118	29
A-7.	Photomicrographs for BOM plate no. 119	30
A-8.	Photomicrographs for BOM plate no. 120	31
B-1.	$V_S - V_R$ plot for 100-mm annealed Ti-6A1-4V vs. 65 g, L/D = 10 X21	37
B-2.	$V_S - V_R$ plot for 104-mm STA Ti-6A1-4V vs. 65 g, L/D = 10 DU	40

INTENTIONALLY LEFT BLANK.

LIST OF TABLES

Table		Page
1.	Typical Chemical Compositions for Ti-6A1-4V and RHA	4
2.	Typical Mechanical Properties for Ti-6A1-4V and RHA	4
3.	Typical Mechanical Properties for Model Scale Projectiles	7
4.	Semi-Infinite Penetration Into RHA	8
5.	Limit Velocity Data for RHA	9
6.	Semi-Infinite Penetration Results for Annealed Ti-6A1-4V vs. L/D = 10 X21	10
7.	Semi-Infinite Penetration Results for STA Ti-6A1-4V vs. L/D = 10 DU	10
8.	Limit Velocity Results for Titanium	12
A-1.	Ti-6A1-4V Plates Utilized for Test Program	21
A-2.	Charpy Impact Results in Transverse/Longitudinal (TL) Direction for Ti-6A1-4V Plates at –40° C	22
A-3.	Mechanical Properties for BOM Plate No. 115	23
A-4.	Mechanical Properties for BOM Plate No. 118	23
B-1.	Semi-Infinite Penetration Performance of Tungsten Rods vs. RHA and Ti-6A1-4V	35
B-2.	Finite Plate Thickness Perforation Performance of Tungsten Rods vs. Ti-6A1-4V	36
B-3.	Semi-Infinite Penetration Performance of Depleted Uranium Rods vs. RHA and Ti-6A1-4V	38
B-4.	Finite Plate Thickness Perforation Performance of Depleted Uranium Rods vs. Ti-6A1-4V	39

INTENTIONALLY LEFT BLANK.

1. INTRODUCTION

Titanium alloys have long been used for reducing system weight in airframe structure and jet engine components. The high cost of titanium, however, has historically prevented its use in military ground vehicles. In recent years, the cost of titanium has fallen relative to the cost of composite and ceramic armors, and titanium is now a valid option for some armor applications.

As early as 1950, Pitler and Hurlich (1950) noted that titanium alloys showed promise as armors against small arms projectiles. By the early 1960s, Sliney (1964) presented ballistic performance data for Ti-6Al-4V alloy that demonstrated significant weight reductions over steel armors for a variety of small arms threats. Little follow-on work with larger threats was conducted due to the prohibitive cost of the titanium. Currently, this lack of baseline titanium ballistic performance data against modern tungsten alloy (WA) and depleted uranium (DU) alloy penetrators is an additional impediment to the consideration of titanium by armor designers.

To provide this armor performance baseline, the U.S. Army Tank-Automotive Research, Development, and Engineering Center, Warren, MI, funded the Weapons Technology Directorate (WTD) of the U.S. Army Research Laboratory (ARL), Aberdeen Proving Ground, MD, to conduct a ballistic evaluation of thick titanium plates with WA and DU penetrators during 1990–1992. The U.S. Department of Interior Bureau of Mines (BOM) at Albany, OR, was funded to purchase 76.2-mm–101.6-mm-thick Ti-6Al-4V plates manufactured to the common MIL-T-9046J specification. The BOM performed heat treating, conducted inspection and metallography, and then shipped the plates to WTD for ballistic testing.

Although the BOM provided both annealed and solution treated and aged (STA) plates, the quantities were not sufficient to allow both heat treatments to be tested with both penetrators. The two choices were either to fire only one penetrator against both types of titanium or to test each penetrator against a different type of titanium. Consequently, since the objective of the test was to evaluate penetration and perforation performance of both the tungsten and DU penetrators, the STA plates were tested with only the DU rods and the annealed plates were tested with only the tungsten X21 rods.

2. BACKGROUND

Titanium can exist in a hexagonal close-packed crystal structure (known as the alpha phase) and a body-centered cubic structure (known as the beta phase). In unalloyed titanium, the alpha phase is stable at all temperatures up to 882° C where it transforms to the beta phase. This transformation temperature is known as the beta transus temperature. The beta phase is stable from 882° C to the melting point (Donachie 1989).

As alloying elements are added to pure titanium, the phase transformation temperature and the amount of each phase present change. Alloy additions to titanium, except tin and zirconium, tend to stabilize either the alpha or beta phase. Ti-6Al-4V, the most common titanium alloy, contains mixtures of alpha and beta phases and is therefore classified as an alpha-beta alloy. The aluminum is an alpha stabilizer, which stabilizes the alpha phase to higher temperatures, and the vanadium is a beta stabilizer, which stabilizes the beta phase to lower temperatures. The addition of these alloying elements raises the beta transus temperature to approximately 996° C. Alpha-beta alloys, such as Ti-6Al-4V, are of interest for armor applications because they are generally weldable, heat treatable, and moderate to high in strength (Donachie 1989).

Ti-6Al-4V can be ordered to a variety of commercial and military specifications. Plates manufactured to aerospace specification MIL-T-9046J were selected for this analysis because this material was readily available. This specification defines alloy chemistry ranges, processing, minimum mechanical properties, and handling and inspection procedures; but it does not define ballistic requirements. Since large plates were not required, the BOM purchased scrap pieces that had been trimmed from full-size plates after rolling. As a result, the order was completed quickly and the cost was reduced. All plates were provided by OREMET of Albany, OR, and had been rolled at temperatures below the beta transus. The BOM assigned identification numbers to each plate upon receipt, and these numbers are used in this report. The BOM then provided final heat treatments, as well as furnished micrographs and mechanical property information, which can be found in Appendix A.

Heat treatments can produce different microstructures and properties in Ti-6Al-4V. Plates 102 and 104 were annealed at 816° C for two hours and then air cooled. The micrographs show a coarse plate-like alpha (white) and intergranular beta microstructure. A low-temperature anneal, such as this, is generally used throughout the titanium industry to relieve rolling stresses while slightly reducing strength.

The STA plates, Nos. 115–120, were heated at 954° C for 2 hr, water quenched, aged at 593° C for 6 hr, and then air cooled. Since 954° C is below the beta transus, only part of the alpha in the prior structure dissolved to form beta. The undissolved alpha is seen as the equiaxed, white, primary phase in the micrographs. The primary alpha is surrounded by transformed beta, consisting of fine acicular alpha in beta. Alpha was also precipitated at the prior grain boundaries and can be seen in the micrographs. Quenching and aging in the alpha plus beta region is considered to provide the best combination of strength and toughness.

Rolled homogeneous armor (RHA) (MIL-A-12560) steel is always used as a baseline with which to compare the ballistic performance of a new armor material. Consequently, general chemical compositions and mechanical properties for Ti-6Al-4V and RHA are provided in Tables 1 and 2, respectively. Note that the RHA properties in this table were for plate thicknesses ranging from 38 mm to 152 mm. The mechanical properties of RHA vary as a function of plate thickness due to differences in thermomechanical processing. A 38-mm-thick RHA plate has higher strength and hardness than a 152-mm-thick plate. The measured Ti-6Al-4V mechanical properties in Appendix A met or exceeded the minimum properties listed in Table 2.

3. TEST METHODOLOGY

The penetrators were fired from a laboratory gun consisting of a 37-mm breech assembly with a 26-mm smoothbore barrel. A custom-built polypropylene sabot system was used to launch the projectiles. The target was positioned 1.5 m in front of the gun. The propellant weight was adjusted to achieve desired striking velocities. Ballistic results for projectiles impacting the target with 2° or greater of total yaw were disregarded. An orthogonal flash radiographic system (Grabarek and Herr 1966) was used to measure projectile velocity, pitch, and yaw prior to striking the target.

Semi-infinite penetration testing and limit velocity perforation testing were both performed for 0° obliquity plates. Semi-infinite testing involves shooting a penetrator into a thick stack of plate such that no deformation or bulging of the sides and back surface of the plate occur. This measures the pure penetration of the projectile into the material without rear surface breakout effects. Limit velocity perforation testing involves varying the impact velocity against a single thickness of plate and measuring the exit velocity of the residual penetrator. The limit velocity (V_L) is defined as the critical velocity at

Table 1. Typical Chemical Compositions for Ti-6Al-4V and RHA

Element	Ti-6Al-4V, MIL-T-9046J (Donachie 1989)	RHA, MIL-A-12560 (Benck 1976)
Titanium	Balance Remaining	None Detected
Carbon	0.08% max.	0.26–0.27%
Manganese		0.27%
Phosphorus		0.001%
Sulfur		0.008%
Silicon		0.15%
Nickel		3.0–3.5%
Copper		0.05–0.07%
Chromium		1.0–1.4%
Vanadium	3.5–4.5%	<0.01%
Molybdenum		0.10–0.25%
Aluminum	5.50–6.75%	<0.03%
Nitrogen	0.05% max.	
Hydrogen	125 ppm max.	
Oxygen	0.20% max.	
Yttria	50 ppm max.	
Other	0.4% max.	
Iron	0.3% max.	Balance Remaining

Table 2. Typical Mechanical Properties for Ti-6Al-4V and RHA

Property	Ti-6Al-4V, MIL-T-9046J (Donachie 1989)	RHA, MIL-A-12560 (Benck 1976)
Ult. Tens. Str. (MPa)	900 min	794–951
Yield Strength (MPa)	830 min	651–826
% Elongation	10 min	11–22
Hardness (BHN)	321–364	241–331
Density (g/cm^3)	4.45	7.85

which the target is just perforated (i.e., the residual velocity is zero). The residual velocity of the penetrator was measured using an additional pair of x-ray tubes behind the target. A schematic of the test setup is shown in Figure 1. The V_L was calculated using the Lambert and Jonas methodology (Lambert and Jonas 1976) to fit the striking velocity/residual velocity (V_S/V_R) data pairs to the following equation:

$$V_R = A\left(V_S{}^P - V_L{}^P\right)^{\frac{1}{P}}, \tag{1}$$

where A, P, and V_L are determined by a nonlinear regression (curve fitting) procedure. The limit velocity determination generally requires 10 shots.

For both test penetrators, the performance of the titanium plate was compared to the 0° obliquity baseline performance of RHA by using areal densities to calculate a measure known as mass effectiveness (E_M). Areal density is defined as the thickness of material perforated (or depth penetrated) times the density of this material. The E_M is defined as the RHA areal density required to defeat a penetrator

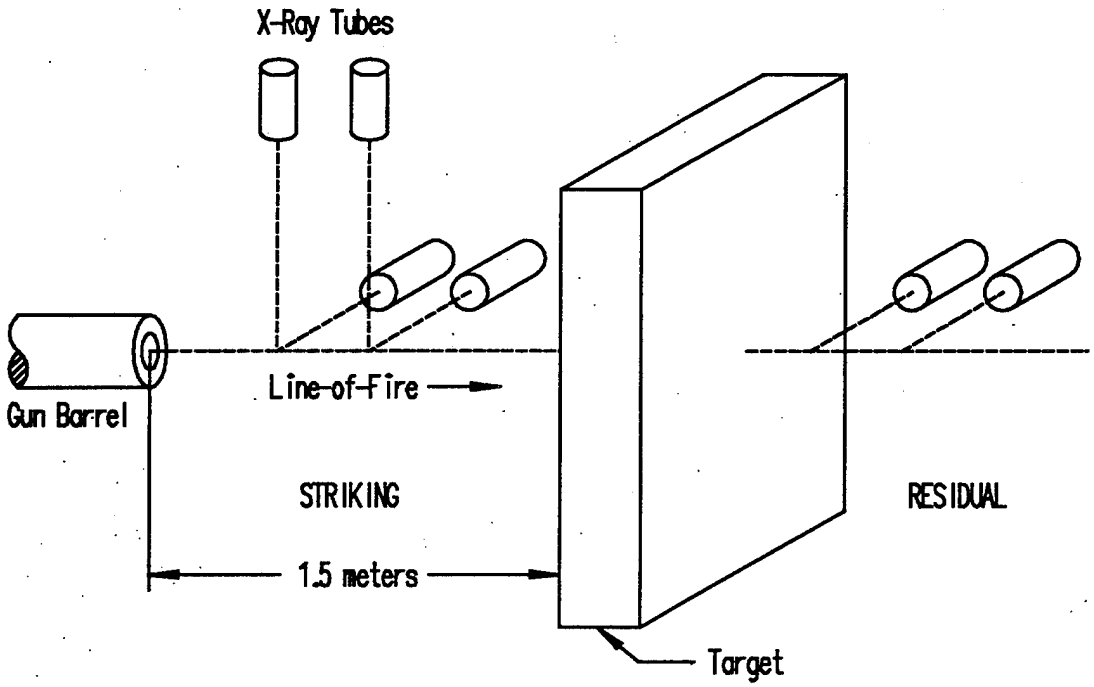

Figure 1. Schematic of test setup.

divided by the areal density of the armor under investigation. In the case of limit velocity testing, the denominator is the areal density of the titanium plate and the numerator is the RHA areal density corresponding to the same obliquity and limit velocity as the titanium. For semi-infinite penetration at a given velocity, the numerator is the product of the density and the depth of penetration into RHA; the denominator is the product of the density and the depth of penetration into a stack of titanium plates.

By definition, the E_M of RHA steel equals 1.0. An E_M greater than 1.0 indicates increased ballistic performance as compared to RHA; an E_M less than 1.0 indicates decreased ballistic performance as compared to RHA.

4. TEST PENETRATORS

Testing was performed with tungsten alloy (WA) and depleted uranium (DU) model scale penetrators. These penetrators were commonly used for screening ceramics and were available for use in this test series. A sketch of these penetrators is provided in Figure 2. The WA penetrators were produced by Teledyne Firth Sterling of Lavergne, TN, using a tungsten/nickel/iron alloy known as X21. The DU penetrators were produced by Nuclear Metals Incorporated of Concord, MA, using a depleted uranium/ titanium alloy. Table 3 lists composition and mechanical property information on the L/D = 10 X21 and the L/D = 10 DU penetrators. Note that because the densities were different, the dimensions of the two rods were slightly different in order to maintain a constant L/D ratio and a constant mass.

The perforation and penetration performance of these X21 and DU penetrators into RHA at 0° obliquity had been collected for previous test programs. The semi-infinite penetration data for RHA are provided in Table 4. Since the relationship between RHA penetration depth and penetrator velocity appeared to be linear over the velocity regimes tested, a linear regression analysis was performed to obtain penetration equations for the X21 and DU rods. These penetration equations for 0° obliquity, Equations 2 and 3, were then used for calculating RHA penetration for purposes of determining E_M.

$$\text{L/D = 10 X21 Penetration into RHA:} \quad P = 0.084V - 53.9, \tag{2}$$

$$\text{L/D = 10 DU Penetration into RHA:} \quad P = 0.070V - 29.7, \tag{3}$$

where P is the depth of penetration in millimeters and V is the striking velocity in m/s.

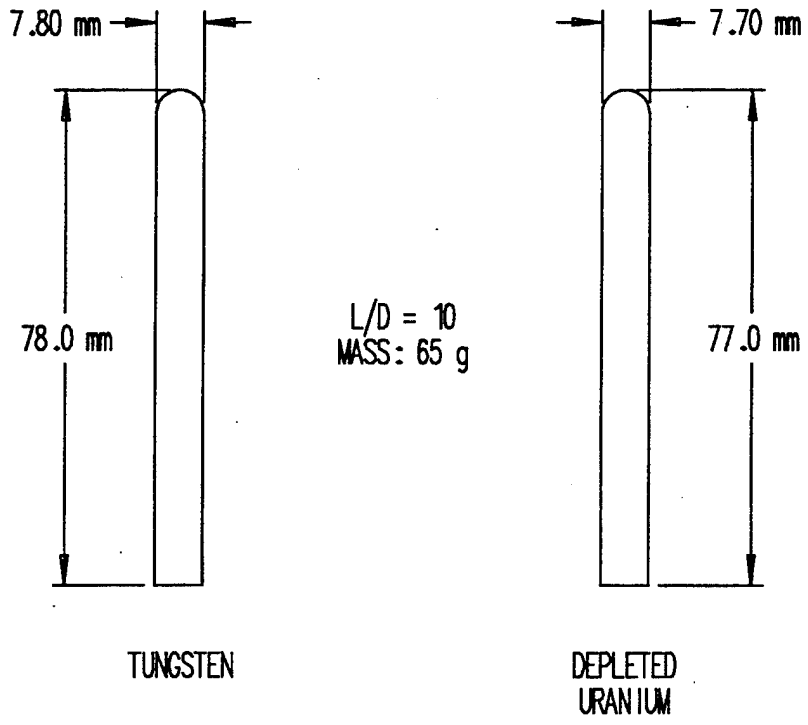

Figure 2. Model scale penetrators.

Table 3. Typical Mechanical Properties for Model Scale Projectiles

	Penetrator Type	
	Tungsten Alloy	Depleted Uranium
Designation	L/D = 10 X21	L/D = 10 DU
Alloy	93% W - 5% Ni - 2% Fe	DU - 0.75% Ti
Density (g/cm^3)	17.7	18.6
Hardness (Rc)	40–45	38–44
Yield Strength (MPa)	1,200	800
Ultimate Tensile Strength (MPa)	1,280	1,380
Elongation (%)	8	12

Table 4. Semi-Infinite Penetration Into RHA

L/D = 10 X21 Penetrator		L/D = 10 DU Penetrator	
Striking Velocity (m/s)	Depth of Penetration (mm)	Striking Velocity (m/s)	Depth of Penetration (mm)
1,096	37	1,047[a]	43
1,267	55	1,070[a]	44
1,387	63	1,209[a]	54
1,503	71	1,264[a]	61
1,507	74	1,550[a]	78
1,518	73	1,629	88
1,522	76	1,747[a]	91
1,571	79	1,897[a]	101
1,671	86		

[a] Farrand and Magness, to be published.

The limit velocity data for RHA, provided in Table 5, were used to determine the relationship between RHA plate thickness and the perforation limit velocity. Since this relationship appeared to be linear over the velocity regimes tested, a linear regression analysis was performed to obtain perforation equations for the X21 and DU rods. These perforation equations for 0° obliquity, Equations 4 and 5, were then used for calculating RHA limit thickness for purposes of determining E_M.

$$\text{L/D = 10 X21 Perforation of RHA:} \quad T = 0.086V_L - 49.6, \tag{4}$$

$$\text{L/D = 10 DU Perforation of RHA:} \quad T = 0.081V_L - 33.6, \tag{5}$$

where T is the thickness of the plate in millimeters and V_L is the limit velocity in m/s.

Table 5. Limit Velocity Data for RHA

L/D = 10 X21		L/D = 10 DU	
RHA Plate Thickness (mm)	Limit Velocity (m/s)	RHA Plate Thickness (mm)	Limit Velocity (m/s)
50.8	1,166	50.8[b]	1,053
76.2[a]	1,461	76.2[a]	1,322
		101.6[b]	1,674

[a] Magness (1992).
[b] Farrand (1994).

5. RESULTS

The BOM furnished the Ti-6Al-4V plates for testing with the X21 and DU penetrators. The BOM purchased the plates from OREMET of Albany, OR, and performed all subsequent processing. As mentioned earlier, the BOM provided both annealed and STA plates, but the quantities were not sufficient to allow both heat treatments to be tested with both penetrators. Consequently, the STA plates were tested with only the DU rods, while the annealed plates were tested with only the X21 rods.

Semi-infinite stacks of titanium plate at 0° obliquity were shot with both penetrators, and the results are listed in Tables 6 and 7. Detailed firing data are furnished in Appendix B. Tables 6 and 7 list the depth of penetration into the stack of titanium plates and the areal density of the titanium. The RHA equivalent penetration was calculated using Equations 2 and 3 for the X21 and DU rods, respectively. The E_M numbers started high (1.7–1.8) at 1,000–1,100 m/s and appeared to fall to a minimum value (1.4–1.5) around 1,600 m/s. For the DU rods, where the test velocity significantly exceeded 1,600 m/s, the E_M numbers appeared to increase again.

Since the penetration data appeared linear, a linear regression was performed and Equations 6 and 7 were obtained for titanium semi-infinite penetration at 0° obliquity:

$$\text{L/D = 10 X21 Penetration into Ti-6Al-4V:} \quad P = 0.108V - 81.7, \tag{6}$$

$$\text{L/D = 10 DU Penetration into Ti-6Al-4V:} \quad P = 0.095V - 56.7, \tag{7}$$

where P is the depth of penetration in millimeters and V is the striking velocity in m/s.

Table 6. Semi-Infinite Penetration Results for Annealed Ti-6Al-4V vs. L/D = 10 X21

Striking Velocity (m/s)	Depth of Penetration (mm)	Areal Density (kg/m^2)	RHA Equivalent Penetration (mm)	RHA Areal Density (kg/m^2)	E_M
1,079	36.5	162	36.7	288	1.78
1,344	60.0	267	59.0	463	1.73
1,506	78.0	347	72.6	570	1.64
1,579	93.5	416	78.7	618	1.49
1,672	98.0	436	86.5	679	1.56

Table 7. Semi-Infinite Penetration Results for STA Ti-6Al-4V vs. L/D = 10 DU

Striking Velocity (m/s)	Depth of Penetration (mm)	Areal Density (kg/m^2)	RHA Equivalent Penetration (mm)	RHA Areal Density (kg/m^2)	E_M
1,111	49.5	220	48.1	378	1.72
1,161	50.0	223	51.6	405	1.82
1,325	67.5	300	63.1	495	1.65
1,452	81.0	360	71.9	564	1.57
1,537	89.0	396	77.9	612	1.55
1,627	105.0	467	84.2	661	1.42
1,709	109.0	485	89.9	706	1.46
1,770	109.6	488	94.2	739	1.51
1,947	122.7	546	106.6	837	1.53

At approximately 1,100 m/s striking velocity, the depth of penetration into RHA and titanium is approximately equal. As the striking velocity increases, however, both the X21 and the DU rods penetrate deeper into the titanium than into the RHA. Also, the performance of the annealed and STA plates seemed comparable based upon E_M numbers. Additional testing is required to conclusively prove that the performance of both heat treatments is the same.

In order to obtain penetration depths, the titanium blocks were sectioned. In most cases, the penetration cavity was free from debris, but on shot no. 2640 the residual tungsten penetrator was still in the plate. Figure 3 is a photograph of the sectioned and polished impact crater for shot no. 2640. The rear surface of the titanium plate is located at the bottom of the picture. The remaining tungsten penetrator is visible at the bottom of the crater. Note that the original flat rear surface of the penetrator is still intact. Behind the penetrator, the cavity is clogged with a mixture of penetrator and target debris. A zone of shear failures in the titanium is visible around the perimeter of this main channel. Farrand (1991) provides a detailed discussion of this type of shear failure in semi-infinite penetration.

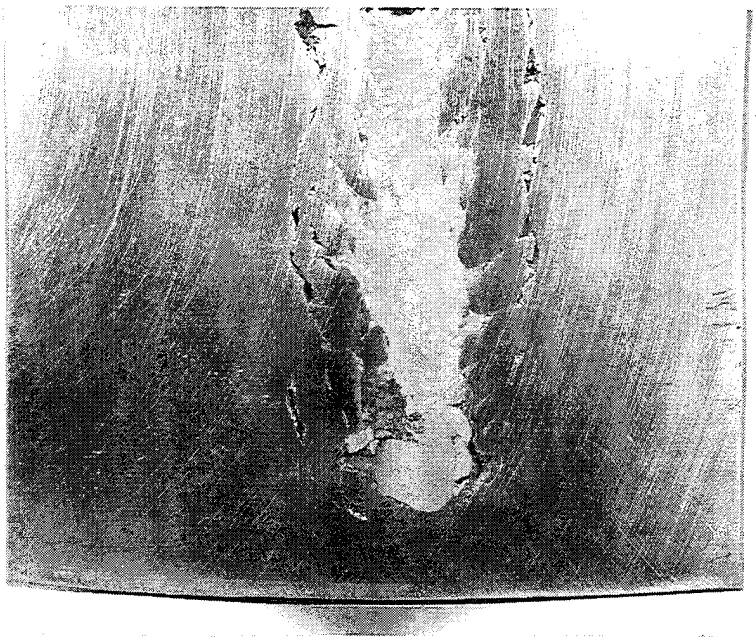

Figure 3. Photograph of sectioned impact crater of tungsten penetrator into annealed T-6Al-4V plate (shot no. 2640).

Finite thickness titanium plate testing was also performed at 0^{o} obliquity with both penetrators in order to obtain limit velocities. Table 8 is a summary of these results; the detailed firing data for all of these shots is furnished in Appendix B. The limit velocity was calculated by performing a least-squares nonlinear regression on Equation 1. The RHA equivalent thickness was calculated using Equations 4 and 5 and the limit velocity determined for the titanium. The E_M performance of the X21 rod vs. the

Table 8. Limit Velocity Results for Titanium

Penetrator	Plate Thickness (mm)	Areal Density (kg/m^2)	Limit Velocity (m/s)	RHA Equivalent Thickness (mm)	RHA Areal Density (kg/m^2)	E_M
L/D = 10 X21	100	445	1,559	84.5	663	1.5
L/D = 10 DU	104	463	1,517	89.3	701	1.5

annealed plate and the DU rod vs. the STA plates seemed to be comparable; however, additional testing is required to conclusively prove that the performance of both heat treatments is the same.

Figure 4 provides a graph of X21 penetration and perforation data for both titanium and RHA. Figure 5 provides the same data for DU. The depths of penetration (for semi-infinite testing) and limit thicknesses (for limit velocity testing) have been converted to areal densities for these plots.

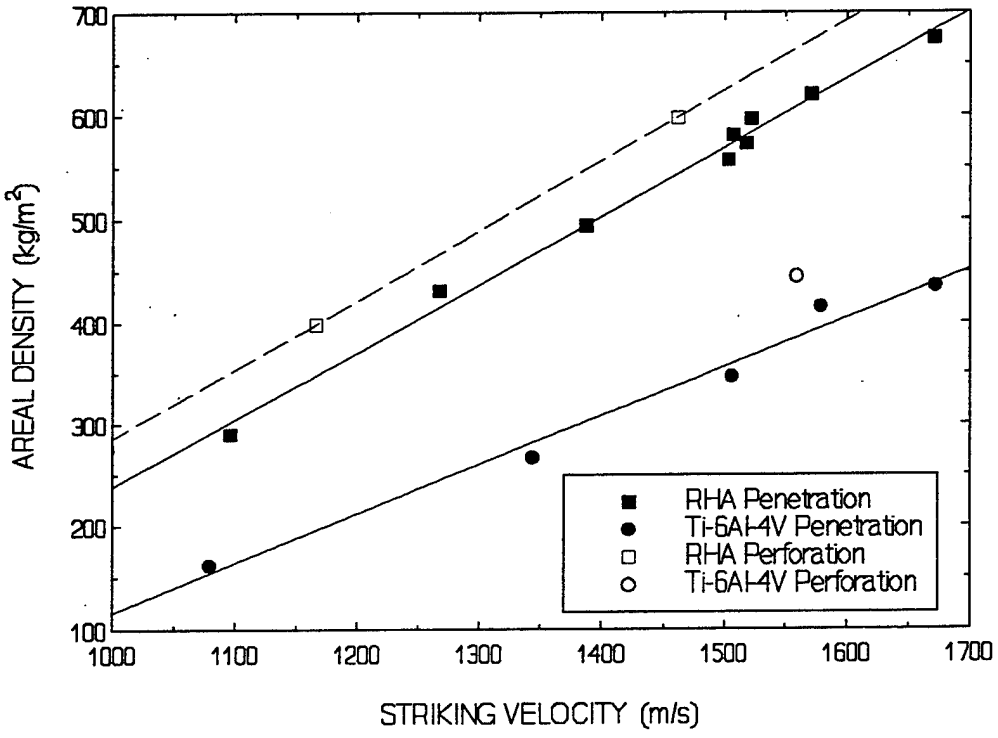

Figure 4. Penetration and perforation results for L/D = 10 X21.

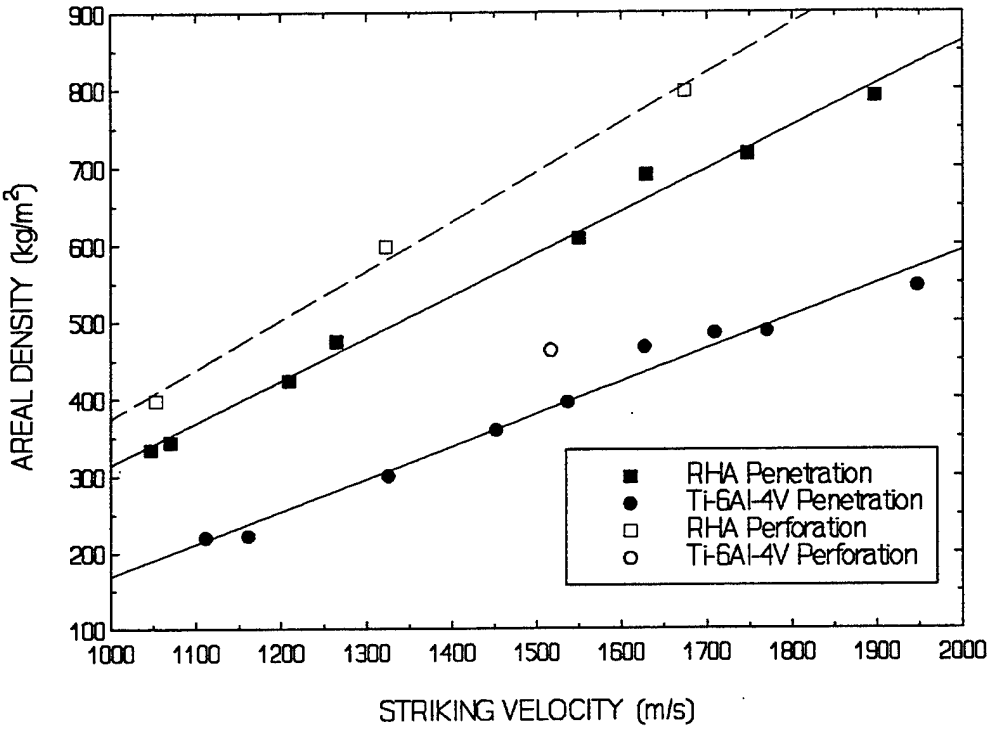

Figure 5. Penetration and perforation results for L/D = 10 DU.

Finite plate testing also permitted observation of hole size and breakout behavior of RHA and Ti-6Al-4V. For both penetrators, the RHA rear surface failed by a process of ductile bulging followed by plugging. Plugging is the failure of the plate when a cylinder of RHA is ejected from the rear surface of the plate. The main penetration channel diameter averaged 10–11 mm for both the DU and X21 rods, respectively. The exit hole, where the plug was ejected, was 19–20 mm diameter on average. A typical exit hole in RHA is shown in Figure 6.

By contrast, the Ti-6Al-4V plates failed by rear surface spalling, the ejection of a disk several times the diameter of the penetration channel. The average penetration channel diameter for both rods was 19 mm. For the annealed Ti-6Al-4V vs. the X21 rod, the average spall diameter was 43 mm. The spall diameter averaged 45 mm for the STA titanium vs. the DU rods. Typical exit holes for annealed and STA Ti-6Al-4V are shown in Figures 7 and 8, respectively. Additional testing is required to quantify any differences in spall behavior between the annealed and STA titanium. In all cases, the penetration channel and exit hole diameters for the Ti-6Al-4V were significantly larger than for RHA.

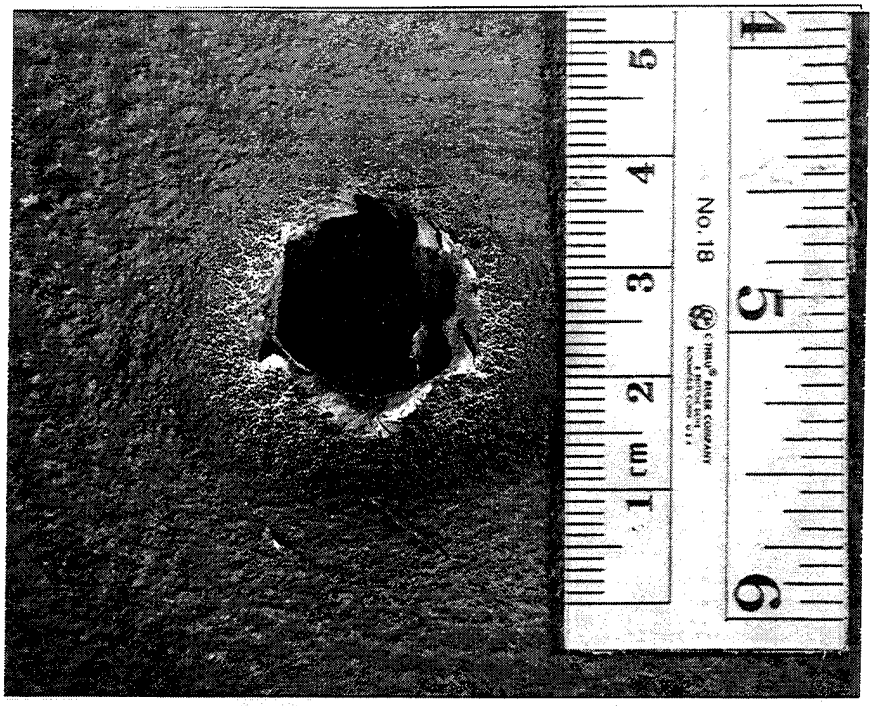

Figure 6. Photograph of typical exit hole in RHA.

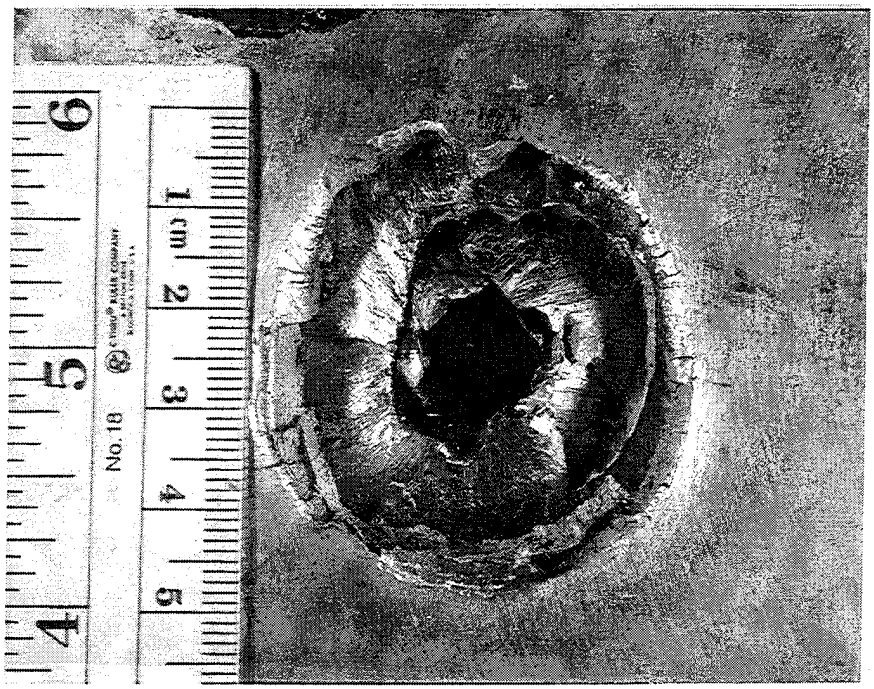

Figure 7. Photograph of typical exit spall in annealed Ti-6Al-4V.

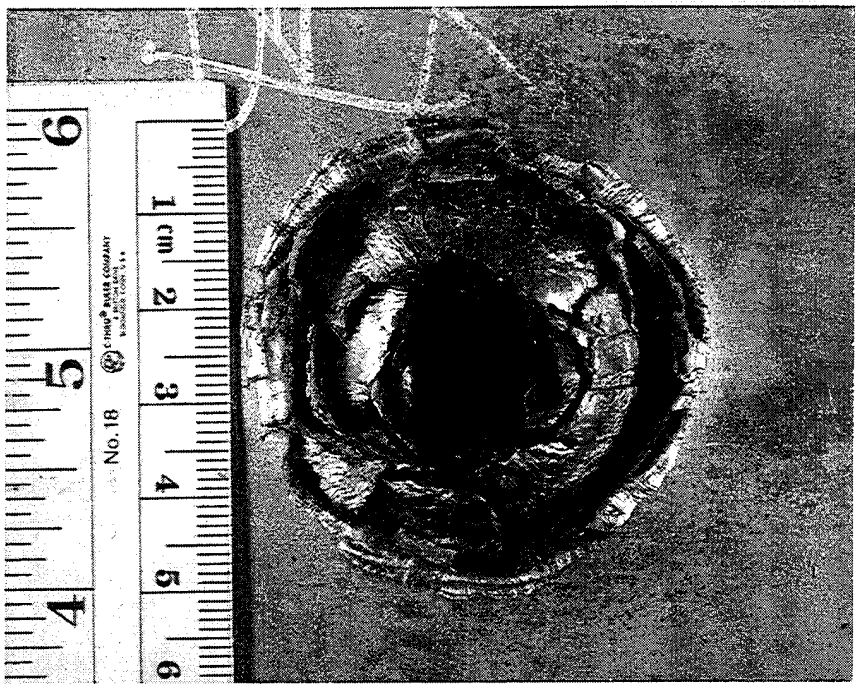

Figure 8. Photograph of typical exit spall in STA Ti-6Al-4V.

6. CONCLUSIONS

The Ti-6Al-4V plates performed surprisingly well compared to RHA based upon E_M calculations. In semi-infinite penetration testing at 0° obliquity, the titanium plates achieved E_Ms of 1.5–1.8 for both tungsten and DU long rod penetrators at velocities from 1,100–1,600 m/s. At approximately 1,100 m/s striking velocity, the depth of penetration into RHA and titanium is approximately equal and results in an E_M of 1.8. As the striking velocity increases to 1,600 m/s, however, the tungsten and DU rods penetrate deeper into the titanium than the RHA and the resulting E_M decreases to 1.5.

The titanium plates also performed well compared to RHA in finite plate thickness limit velocity testing at 0° obliquity. The E_Ms for perforation testing were estimated to be approximately 1.5 for both tungsten and DU rods. When perforated by a long rod penetrator, the titanium tends to fail by spalling while the RHA tends to fail by ductile bulging followed by plugging. In all cases, the penetration channel and exit hole diameters for the Ti-6Al-4V were significantly larger than for RHA. For either Ti-6Al-4V

or RHA, spall liners are recommended for use in armor designs in order to reduce the lethality of behind armor debris in overmatching penetrator impacts.

While testing both types of penetrator against a single heat treatment of titanium would have been ideal, sufficient quantities of plate were not available to accomplish this. However, the performance of the annealed and STA plates seemed comparable based upon E_M numbers. Additional testing is required to conclusively prove that one heat treatment is preferable to the other.

7. REFERENCES

Benck, R. "Quasi-Static Tensile Stress Strain Curves- II, Rolled Homogeneous Armor." BRL-MR-2703, U.S. Army Ballistic Research Laboratory, Aberdeen Proving Ground, MD, November 1976.

Donachie, M. Titanium: A Technical Guide. ASM International, Metals Park, OH, 1989. (ISBN: 0-87170-309-2)

Farrand, T. "Various Target Material Failure Mechanisms Observed for Ballistic Penetrations." BRL-TR-3255, U.S. Army Ballistic Research Laboratory, Aberdeen Proving Ground, MD, August 1991.

Farrand, T. Unpublished ballistic limit data, U.S. Army Research Laboratory, Aberdeen Proving Ground, MD, private communication, 1994.

Farrand, T., and L. Magness. "Model Scale Terminal Ballistic Evaluation of Various Geometry Tungsten Heavy Alloy and Depleted Uranium Alloy Penetration Into Semi-Infinite Armor." U.S. Army Research Laboratory, Aberdeen Proving Ground, MD, to be published.

Grabarek, C., and E. Herr. "X-Ray Multi-Flash System for Measurement of Projectile Performance at the Target." BRL Technical Note 1634, U.S. Army Ballistic Research Laboratory, Aberdeen Proving Ground, MD, September 1966. (AD 807619)

Lambert, J., and G. Jonas. "Towards Standardization in Terminal Ballistic Testing: Velocity Presentation." BRL-MR-1852, U.S. Army Ballistic Research Laboratory, Aberdeen Proving Ground, MD, January 1976. (ADA 021389)

Magness, L. "A Phenomenological Investigation of the Behavior of High-Density Materials Under the High Pressure, High Strain Rate Loading Environment of Ballistic Impact." Doctoral Dissertation, Johns Hopkins University, Baltimore, MD, 1992.

Pitler, R., and A. Hurlich. "Some Mechanical and Ballistic Properties of Titanium and Titanium Alloys." Report No. 401/17, Watertown Arsenal Laboratory, Watertown, MA, March 1950. (ADA 951655)

Sliney, J. "Status and Potential of Titanium Armor." Proceedings of the Metallurgical Advisory Committee on Rolled Armor, AMRA MS 64-04, U.S. Army Materials Research Agency, Watertown, MA, January 1964. (AD 354853)

INTENTIONALLY LEFT BLANK.

APPENDIX A:

MATERIAL PROPERTY DATA FOR TI-6A1-4V PLATES

INTENTIONALLY LEFT BLANK.

Table A-1. Ti-6Al-4V Plates Utilized for Test Program

BOM Plate No.	Thickness (mm)	Lateral Dimensions (mm)	Hardness (BHN)	Heat Treatment
102	97	305 × 305	364	Annealed 2 hr @ 816° C, AC
104	100	229 × 457	364	Annealed 2 hr @ 816° C, AC
114	80	305 × 457	364	STA 2 hr @ 954° C, WQ, 6 hr @ 593° C, AC
115	104	165 × 406	321	STA 2 hr @ 954° C, WQ, 6 hr @ 593° C, AC
116	104	165 × 406	340	STA 2 hr @ 954° C, WQ, 6 hr @ 593° C, AC
117	104	165 × 406	340	STA 2 hr @ 954° C, WQ, 6 hr @ 593° C, AC
118	104	165 × 406	340	STA 2 hr @ 954° C, WQ, 6 hr @ 593° C, AC
119	107	127 × 457	321	STA 2 hr @ 954° C, WQ, 6 hr @ 593° C, AC
120	107	127 × 457	340	STA 2 hr @ 954° C, WQ, 6 hr @ 593° C, AC

AC = Air Cool
STA = Solution Treated and Aged
WQ = Water Quench

Table A-2. Charpy Impact Results in Transverse/Longitudinal (TL) Direction for Ti-6Al-4V Plates at –40° C

BOM Plate No.	Impact Velocity (m/s)	Energy (J)	Avg. Impact Velocity (m/s)	Avg. Energy (J)
102	3.670 3.667 3.670	23.81 12.22 13.16	3.670	16.73
115	3.670 3.664 3.661	18.37 14.06 16.17	3.664	16.20
116	3.661 3.661 3.667	15.12 16.32 13.83	3.664	15.09
117	3.664 3.664 3.667	14.89 14.67 13.91	3.664	14.49
118	3.664 3.667 3.661	14.22 13.08 14.86	3.664	14.05
119	3.661 3.661 3.661	15.62 17.99 15.35	3.661	16.32

Table A-3. Mechanical Properties for BOM Plate No. 115

Direction	UTS MPa (ksi)	YS MPa (ksi)	Elongation (%)	RA (%)
Transverse	971.5 (140.9)	914.2 (132.6)	11.5	—
"	980.4 (142.2)	919.8 (133.4)	10.4	—
"	982.5 (142.5)	919.1 (133.3)	10.4	15.2
Average	978.4 (141.9)	917.7 (133.1)	10.8	15.2

Table A-4. Mechanical Properties for BOM Plate No. 118

Direction	UTS MPa (ksi)	YS MPa (ksi)	Elongation (%)	RA (%)
Transverse	1007 (146.0)	954.9 (138.5)	8.9	19.7
"	1006 (145.9)	938.4 (136.1)	12.8	—
"	980.4 (142.2)	920.5 (133.5)	10.1	—
Average	997.7 (144.7)	937.7 (136.0)	10.6	19.7

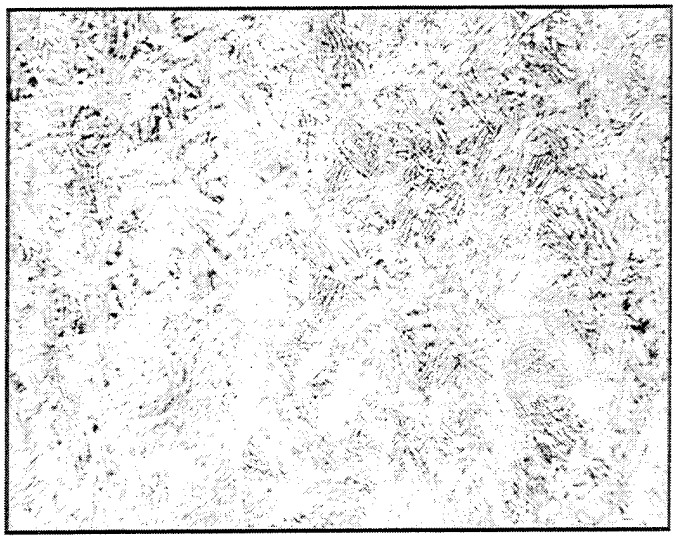

Plate 102, Shot 2639, 50X

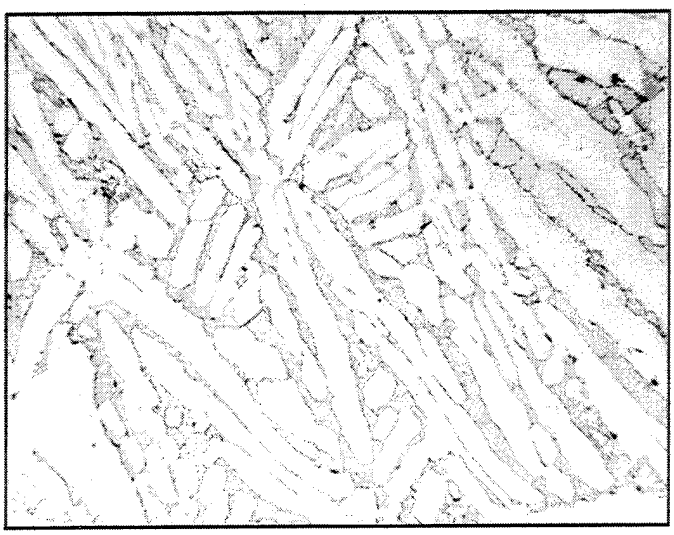

Plate 102, Shot 2639, 500X

Figure A-1. Photomicrographs for BOM plate no. 102.

Plate 104, Shot 2645, 50X

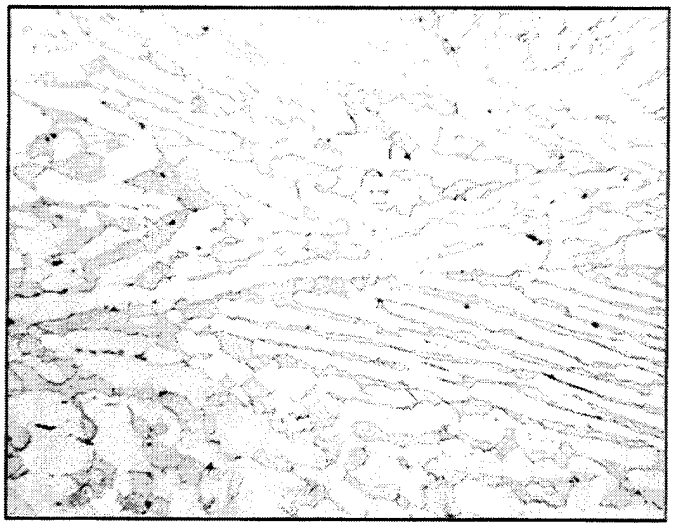

Plate 104, Shot 2645, 500X

Figure A-2. Photomicrographs for BOM plate no. 104.

Plate No. 115 50X

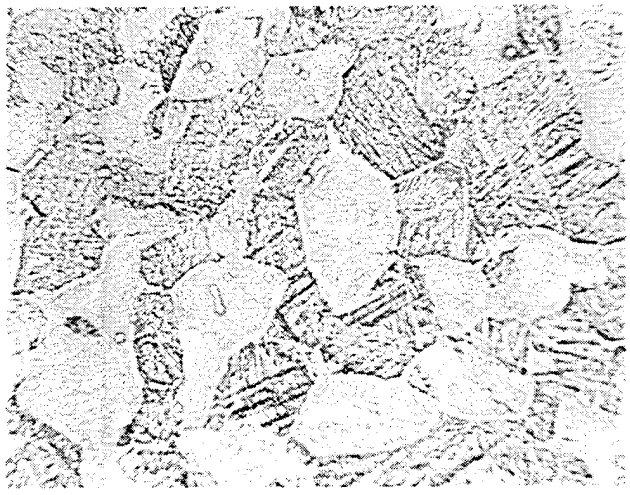

Plate No. 115 500X

Figure A-3. Photomicrographs for BOM plate no. 115.

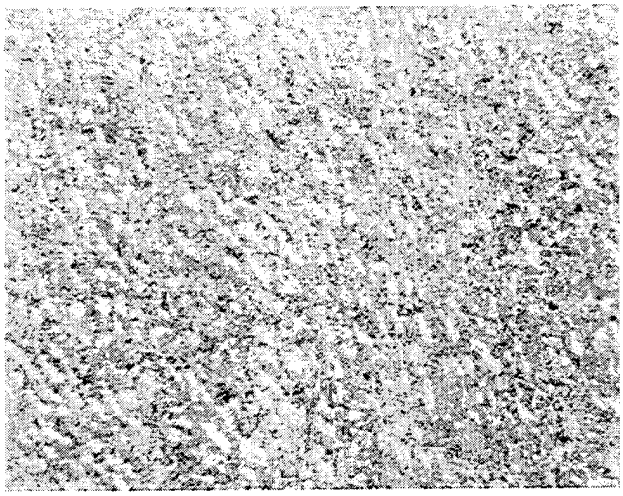

Plate No. 116 50X

Plate No. 116 500X

Figure A-4. Photomicrographs for BOM plate no. 116.

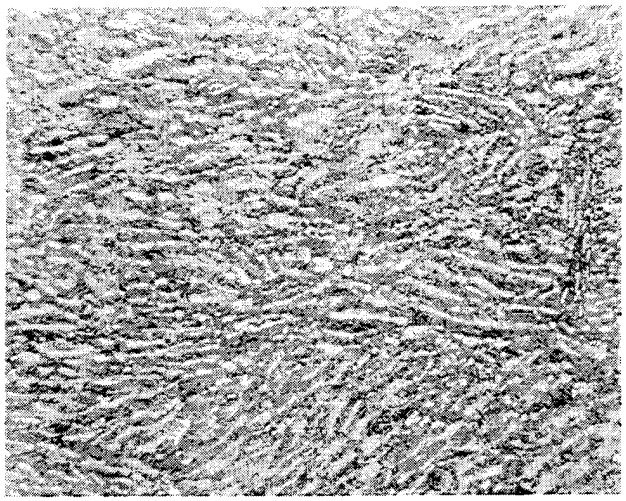

Plate No. 117 50X

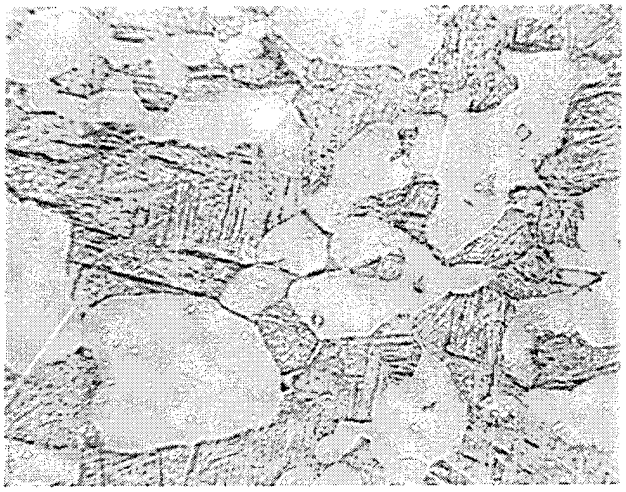

Plate No. 117 500X

Figure A-5. Photomicrographs for BOM plate no. 117.

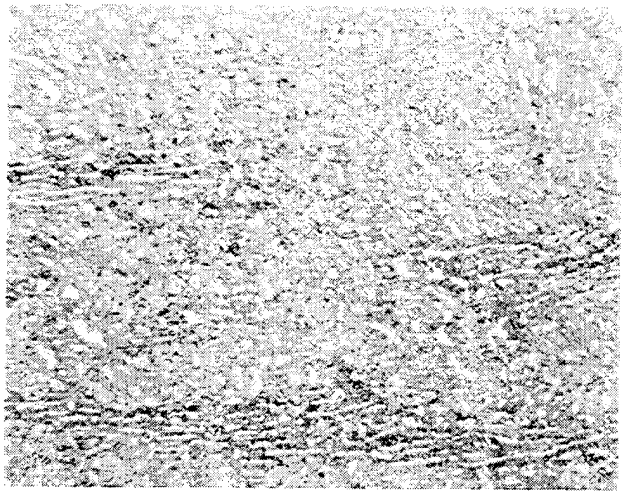

Plate No. 118 50X

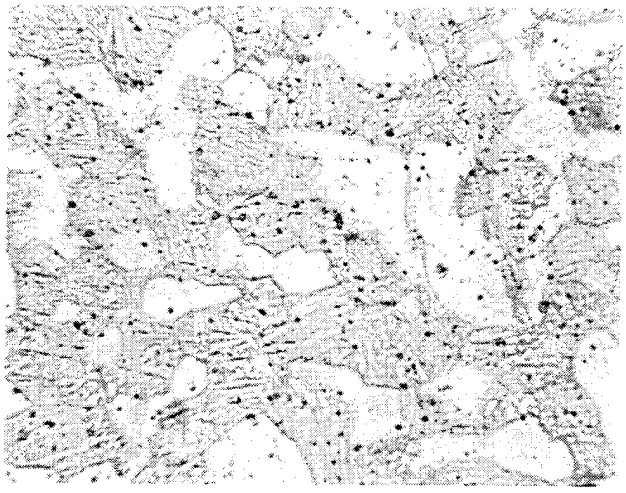

Plate No. 118 500X

Figure A-6. Photomicrographs for BOM plate no. 118.

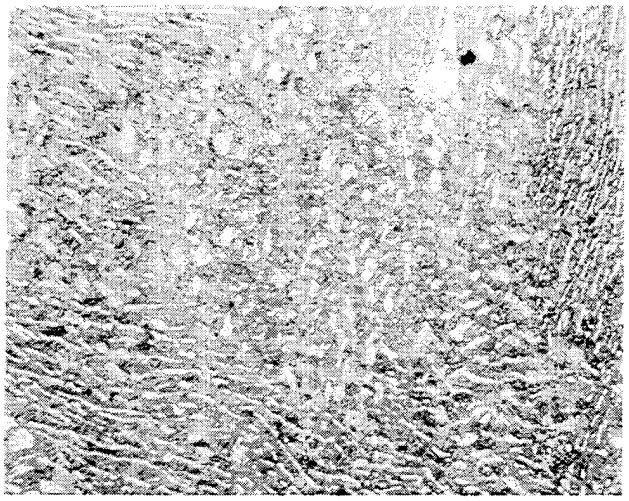

Plate No. 119 50X

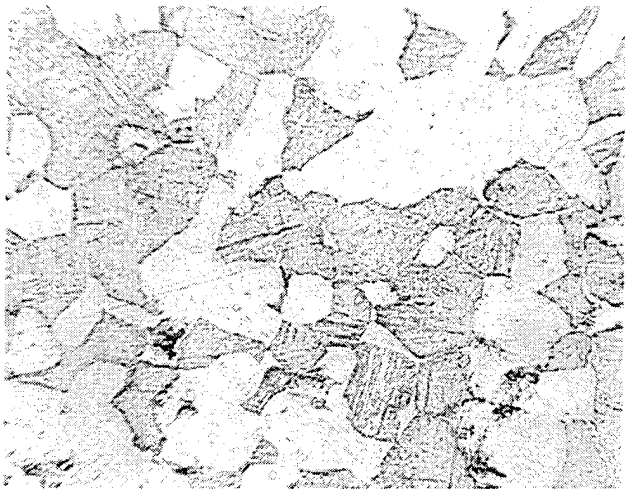

Plate No. 119 500X

Figure A-7. Photomicrographs for BOM plate no. 119.

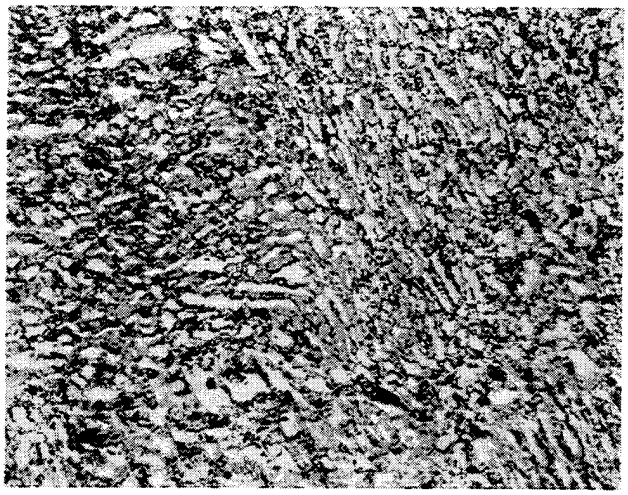

Plate No. 120 50X

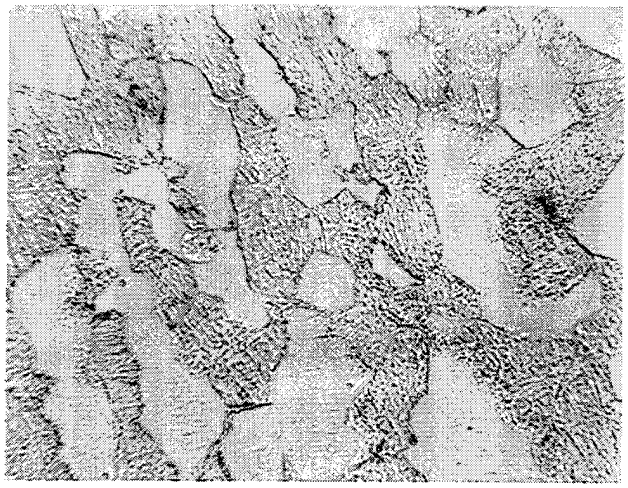

Plate No. 120 500X

Figure A-8. Photomicrographs for BOM plate no. 120.

INTENTIONALLY LEFT BLANK.

APPENDIX B:

DETAILED FIRING DATA FOR Ti-6A1-4V AND RHA

INTENTIONALLY LEFT BLANK.

Table B-1. Semi-Infinite Penetration Performance of Tungsten Rods vs. RHA and Ti-6Al-4V

Penetrator: 65 g, L/D = 10 X21 Plate Obliquity: 0°								
Shot No. (LAT)	Material	Plate No. (BOM)	Thickness (mm)	Hardness (BHN)	V_S (m/s)	Total Yaw (deg)	P_R (mm)	Plate(s) Penetrated
2495	RHA	—	152	255	1,096	1.03	37.0	
2649	RHA	—	152	241	1,267	1.12	55.0	
2651	RHA	—	152	241	1,387	0.79	63.0	
3000	RHA	—	152	255	1,503	1.35	71.0	
2650	RHA	—	152	241	1,507	0.56	74.0	
2931	RHA	—	152	255	1,518	0.25	73.0	
2635	RHA	—	152	255	1,522	1.82	76.0	
3002	RHA	—	152	241	1,571	0	79.0	
2636	RHA	—	152	241	1,671	0.35	86.0	
2641	Ti-6Al-4V	102/104	97/100	364/364	1,079	1.58	36.5	Plate no. 102
2638	Ti-6Al-4V	102/104	97/100	364/364	1,344	0.56	60.0	Plate no. 102
2637	Ti-6Al-4V	102/104	97/100	364/364	1,506	1.27	78.0	Plate no. 102
2640	Ti-6Al-4V	102/104	97/100	364/364	1,579	0.25	93.5	Plate no. 102
2639	Ti-6Al-4V	102/104	97/100	364/364	1,672	1.03	98.0	Plate nos. 102 and 104

Table B-2. Finite Plate Thickness Perforation Performance of Tungsten Rods vs. Ti-6Al-4V

Penetrator: 65 g, L/D = 10 X21

Target: Ti-6Al-4V

Plate Obliquity: 0°

Plate Condition: Annealed

Shot No. (LAT)	Plate No. (BOM)	Thickness (mm)	Hardness (BHN)	V_S (m/s)	Total Yaw (deg)	Result (PP/CP)	V_R (m/s)	L_R (mm)	M_R (g)	P_R (mm)	Comments
2647	104	100	364	1,705	0.00	CP	957	12	10	NA	
2648	104	100	364	1,655	0.56	CP	837	13	11	NA	
2642	104	100	364	1,611	1.03	CP	526	10	8	NA	
2644	104	100	364	1,576	0.79	CP	326	9	8	NA	
2646	104	100	364	1,566	0.75	CP	324	8	7	NA	
2645	104	100	364	1,552	0.00	PP	NA	NA	NA	91	5-mm Bulge w. Star Crack
2643	104	100	364	1,544	0.25	PP	NA	NA	NA	NM	4-mm Bulge w. Star Crack

NA = Not applicable.
NM = Not measured.

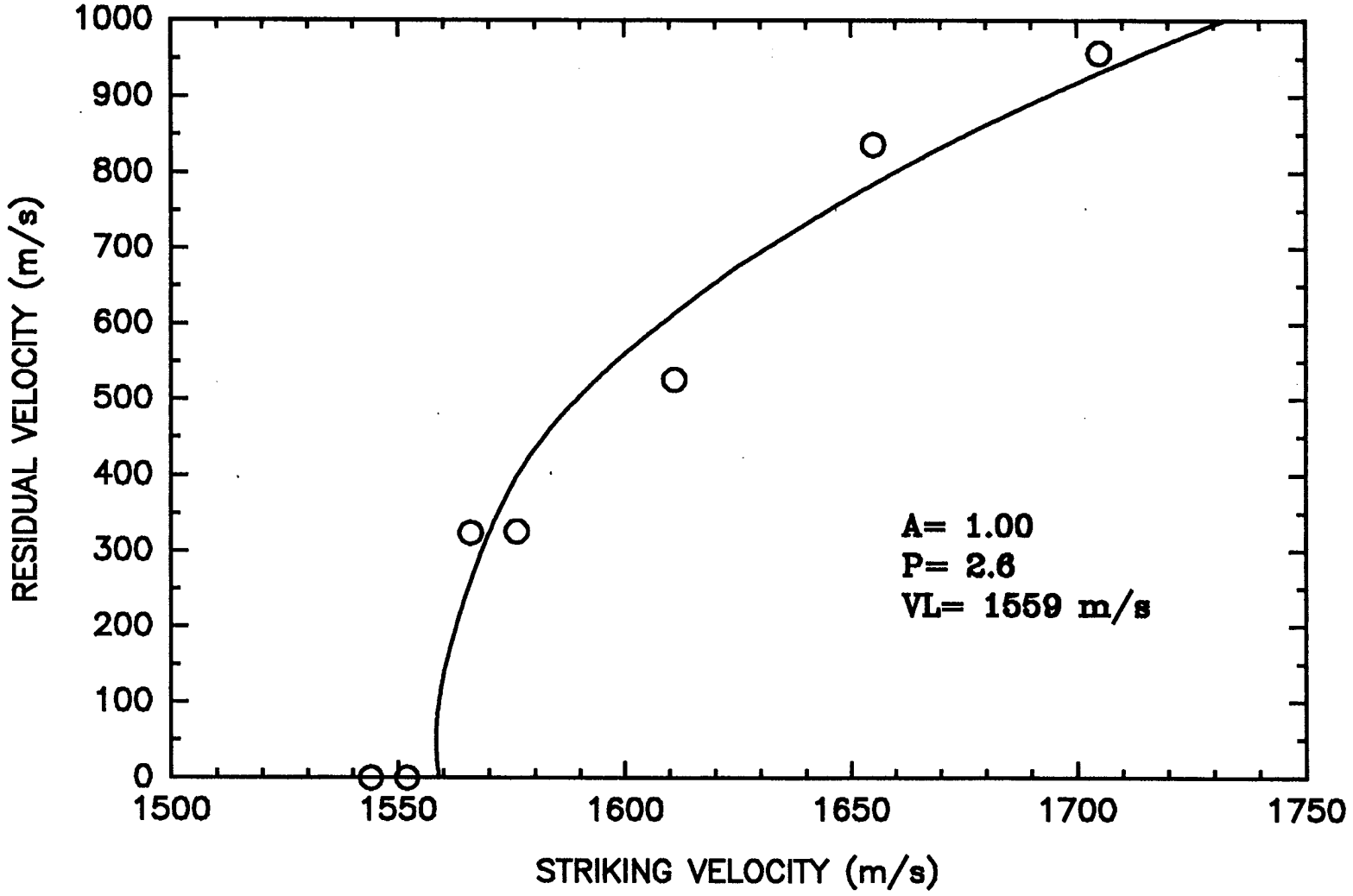

Figure B-1. V_S–V_R plot for 100-mm annealed Ti-6Al-4V vs. 65 g, L/D = 10 X21.

Table B-3. Semi-Infinite Penetration Performance of Depleted Uranium Rods vs. RHA and Ti-6Al-4V

Penetrator: 65 g, L/D = 10 DU Plate Obliquity: 0°								
Shot No. (AMB)	Material	Plate No. (BOM)	Thickness (mm)	Hardness (BHN)	V_S (m/s)	Total Yaw (deg)	P_R (mm)	Plate(s) Penetrated
334	RHA	—	152	255	1,629	0.71	88.0	
972[a]	RHA	—	152	NM	1,550	NM	77.5	
3155[a]	RHA	—	152	255	1,209	0.25	54.1	
3156[a]	RHA	—	152	255	1,070	0.79	43.9	
3159[a]	RHA	—	152	269	1,264	0.90	60.5	
3172[a]	RHA	—	152	241	1,047	1.25	42.7	
3232[a]	RHA	—	152	269	1,897	0.56	100.8	
3233[a]	RHA	—	152	269	1,747	0.25	91.4	
313	Ti-6Al-4V	119/115	107/104	321/321	1,111	1.00	49.5	Plate no. 119
311	Ti-6Al-4V	119/115	107/104	321/321	1,161	0.71	50.0	Plate no. 119
316	Ti-6Al-4V	120/115	107/104	340/321	1,325	1.03	67.5	Plate no. 120
318	Ti-6Al-4V	120/115	107/104	340/321	1,452	1.50	81.0	Plate no. 120
310	Ti-6Al-4V	119/115	107/104	321/321	1,537	0.25	89.0	Plate no. 119
315	Ti-6Al-4V	120/115	107/104	340/321	1,627	0.56	105.0	Plate no. 120
314	Ti-6Al-4V	119/115	107/104	321/321	1,709	1.25	109.0	Plate no. 119/ including 3-mm Bulge
320	Ti-6Al-4V	114/120	80/107	364/340	1,770	0.25	109.6	Plate nos. 114 and 120
317	Ti-6Al-4V	120/115	107/104	340/321	1,947	0.25	122.7	Plate nos. 120 and 115

[a] Farrand and Magness, to be published.

Table B-4. Finite Plate Thickness Perforation Performance of Depleted Uranium Rods vs. Ti-6Al-4V

Penetrator: 65 g, L/D = 10 DU

Target: Ti-6Al-4V

Plate Obliquity: 0°

Plate Condition: Solution Treated and Aged

Shot No. (AMB)	Plate No. (BOM)	Thickness (mm)	Hardness (BHN)	V_S (m/s)	Total Yaw (deg)	Result (PP/CP)	V_R (m/s)	L_R (mm)	M_R (g)	P_R (mm)	Comments
321	115	104.3	321	1,777	0.75	CP	1,301	12	10	NA	
323	116	104.2	340	1,667	1.00	CP	1,043	11	10	NA	
336	118	104.1	340	1,619	1.95	CP	763	6	6	NA	
324	116	104.2	340	1,588	0.75	CP	789	8	7	NA	
338	118	104.1	340	1,575	1.60	CP	688	8	7	NA	
325	116	104.2	340	1,560	1.80	CP	590	8	7	NA	
337	118	104.1	340	1,543	0.25	CP	97	8	7	NA	
326	116	104.2	340	1,528	0.50	CP	272	8	7	NA	
327	116	104.2	340	1,519	1.00	CP	227	6	5	NA	
322	116	104.2	340	1,510	0.90	PP	NA	NA	NA	99	8-mm Bulge w. Cracks
329	117	104.3	340	1,503	1.12	PP	NA	NA	NA	NM	6-mm Bulge w. Cracks
328	116	104.2	340	1,497	0.25	PP	NA	NA	NA	NM	7-mm Bulge w. Cracks

NA = Not applicable.
NM = Not measured.

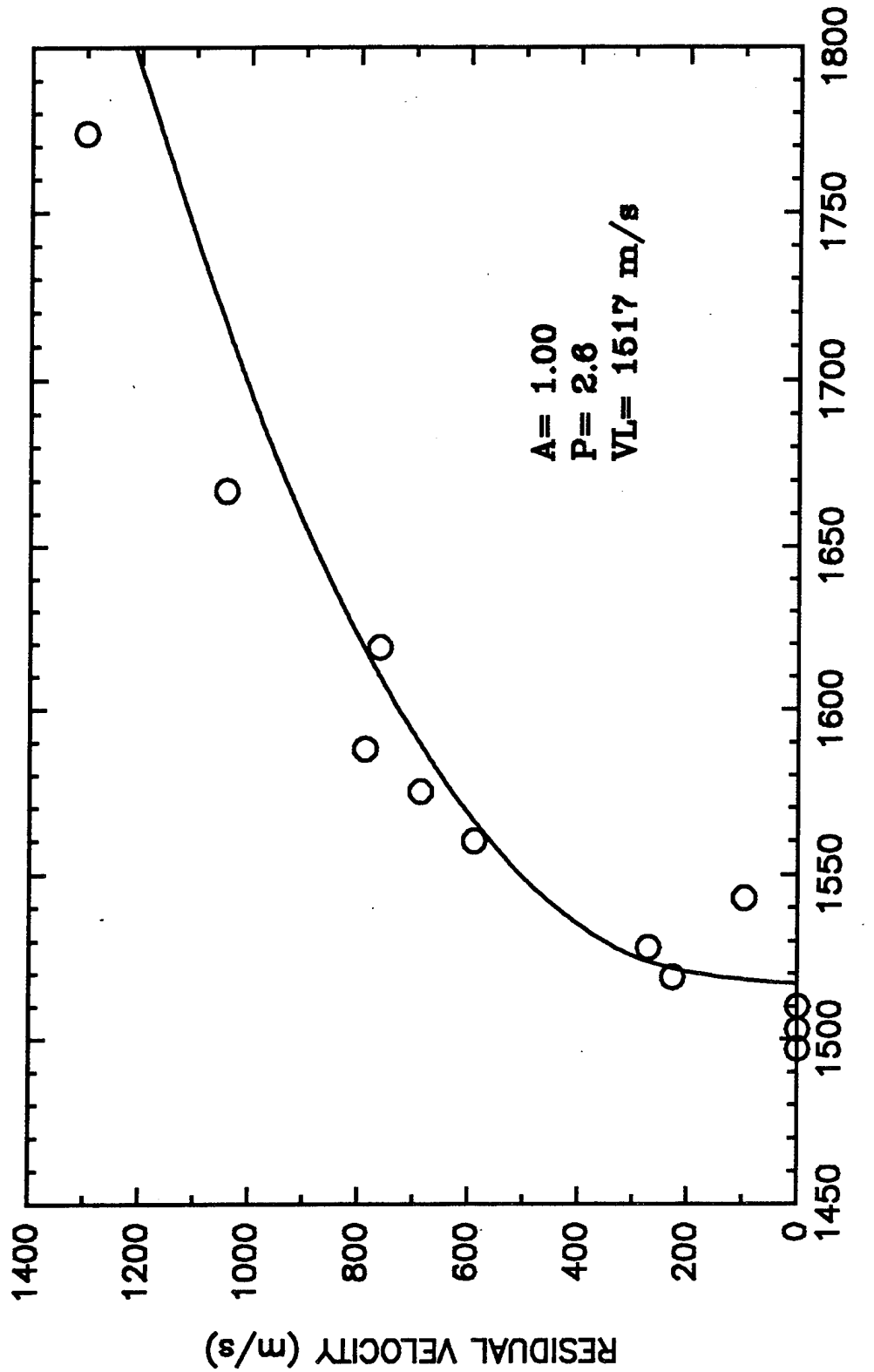

Figure B-2. V_S–V_R plot for 104-mm STA Ti-6Al-4V vs. 65 g, L/D = 10 DU.

NO. OF COPIES	ORGANIZATION
2	DEFENSE TECHNICAL INFO CTR ATTN DTIC DDA 8725 JOHN J KINGMAN RD STE 0944 FT BELVOIR VA 22060-6218
1	DIRECTOR US ARMY RESEARCH LAB ATTN AMSRL OP SD TA 2800 POWDER MILL RD ADELPHI MD 20783-1145
3	DIRECTOR US ARMY RESEARCH LAB ATTN AMSRL OP SD TL 2800 POWDER MILL RD ADELPHI MD 20783-1145
1	DIRECTOR US ARMY RESEARCH LAB ATTN AMSRL OP SD TP 2800 POWDER MILL RD ADELPHI MD 20783-1145
	ABERDEEN PROVING GROUND
2	DIR USARL ATTN AMSRL OP AP L (305)

No. of Copies	Organization
1	HQDA ATTN SARD TR R CHAIT WASHINGTON DC 20310-0103
6	COMMANDER US ARMY TACOM ATTN AMSTA TR S J THOMPSON S GOODMAN D THOMAS D HANSEN AMSTA TR E MATL B ROOPCHAND J OGILVY WARREN MI 48397-5000
2	PROJECT MANAGER SURVIVABILITY SYSTEMS ATTN SFAE ASM ASV T DEAN J ROWE WARREN MI 48397-5000
1	DIRECTOR US ARMY RESEARCH OFFICE ATTN K IYER PO BOX 12211 RESEARCH TRIANGLE PARK NC 27709-2211
1	COMMANDER NATL GROUND INTELLIGENCE CTR ATTN W MARLEY 220 SEVENTH AVE CHARLOTTESVILLE VA 22901-5391
1	CENTRAL INTELLIGENCE AGENCY ATTN OSWR DSD W WALTMAN ROOM 5P0110 NHB WASHINGTON DC 20505
1	DIRECTOR ADVANCED RSRCH PROJECT AGENCY ATTN COL R KOCHER 3701 NORTH FAIRFAX DR ARLINGTON VA 22203-1714

No. of Copies	Organization
1	COMMANDER EUROPEAN RESEARCH OFFICE USARDSG UK ATTN R REICHENBACH PSC 802 BOX 15 FPO AE 09499-1500
4	LAWRENCE LIVERMORE NATL LAB ATTN R GOGOLEWSKI MS L290 R LANDINGHAM L369 D STEINBERG J REAUGH L32 PO BOX 808 LIVERMORE CA 94550
4	LOS ALAMOS NATL LAB ATTN F ADDESSIO M BURKETT E CORT F GAC LOS ALAMOS NM 87545
5	SANDIA NATL LAB ATTN D GRADY MS 0821 M FORRESTAL J ASAY MS 0548 R BRANNON MS 0820 M KIPP MS 0820 PO BOX 5800 ALBUQUERQUE NM 87185
4	INSTITUTE FOR ADVNCD TECH ATTN S BLESS R SUBRAMANIAN T KIEHNE M NORMANDIA PO BOX 202797 AUSTIN TX 78720-2797
1	NAVAL POST GRADUATE SCHOOL ATTN J STERNBERG CODE EW MONTEREY CA 93943
1	INTERNATIONAL RSRCH ASSOCIATES ATTN D ORPHAL 4450 BLACK AVE PLEASANTON CA 94566

No. of Copies	Organization
6	UNITED DEFENSE LP ATTN V HORVATICH J DORSCH R RAJAGOPAL M MIDDIONE R MUSANTE D SCHADE PO BOX 367 SANTA CLARA CA 95103
2	UNIV OF DAYTON RSRCH INSTITUTE KLA14 ATTN A PIEKUTOWSKI N BRAR 300 COLLEGE PARK DAYTON OH 45469-0182
3	SOUTHWEST RSRCH INSTITUTE ATTN C ANDERSON J RIEGEL D LITTLEFIELD 6220 CULEBRA RD SAN ANTONIO TX 78238
1	AERONAUTICAL RSRCH ASSOCIATES ATTN R CONTILIANO PO BOX 2229 50 WASHINGTON RD PRINCETON NJ 08540
1	RMI TITANIUM COMPANY ATTN W LOVE 2950 BIRCH ST BREA CA 92621
1	RMI TITANIUM COMPANY ATTN J WOOD 1000 WARREN AVE NILES OH 44446
2	TIMET ATTN J FANNING P BANIA PO BOX 2128 HENDERSON NV 89009
1	OREGON METALLURGICAL CORP ATTN D HIATT PO BOX 580 ALBANY OR 97321
3	US BUREAU OF MINES ATTN J HANSEN 2 COPIES P TURNER 1450 QUEEN AVENUE SW ALBANY OR 97321-2198
4	GENERAL DYNAMICS LAND SYSTEMS DIVISION ATTN W BURKE W HERMAN D DEBUSSCHER G CAMPBELL PO BOX 2094 WARREN MI 48090-2094
3	CERCOM INC ATTN R PALICKA A EZIS G NELSON 1960 WATSON WAY VISTA CA 92083
1	BRIGGS COMPANY ATTN J BACKOFFEN 2668 PETERSBOROUGH ST HERDON VA 222071-2443
1	APPLIED RSRCH ASSOCIATES INC ATTN J YATTEAU 5941 SO MIDDLEFIELD RD SUITE 100 LITTLETON CO 801123
1	ZERNOW TECHNICAL SERVICES ATTN L ZERNOW 425 W BONITA AVE SUITE 208 SAN DIMAS CA 91773
2	ITG LABORATORIES ATTN C CLINE M WILKENS 702 MARSHALL ST APT 280 REDWOOD CITY CA 94063-1823
1	R J EICHELBERGER 409 W CATHERINE ST BEL AIR MD 21014-3613

No. of Copies	Organization
1	CYPRESS INTERNATIONAL ATTN A CAPONECCHI 1201 E ABINGDON DR ALEXANDRIA VA 22314
1	BATTELLE EDGEWOOD ATTN A RICCHIAZZI 2113 EMMERTON PARK RD EDGEWOOD MD 21040
1	O'GARA HESS AND EISENHARDT ATTN C WILLIAMS 9113 LE SAINT DR FAIRFIELD OH 45014
1	CENTURY DYNAMICS INC ATTN N BIRNBAUM 2333 SAN RAMON VLY BLVD SAN RAMON CA 94583-1613
	ABERDEEN PROVING GROUND
2	DIR USAMSAA ATTN AMXSY-D AMXSY-MP H COHEN
1	CDR USATECOM ATTN AMSTE-TC
1	DIR USAERDEC ATTN SCBRD-RT
1	CDR USACBDCOM ATTN AMSCB-CII
41	DIR USARL ATTN AMSRL-SL-I AMSRL-WT-T W MORRISON AMSRL-WT-TD A DIETRICH JR T FARRAND K FRANK

No. of Copies	Organization
	AMSRL-WT-TC F GRACE R SUMMERS L MAGNESS G SILSBY W DEROSSET AMSRL-WT-TA E HORWATH E RAPACKI JR W GILLICH J DEHN T HAVEL W BRUCHEY JR M BURKINS (10 CPS) W GOOCH N RUPERT J RUNYEON M ZOLTOSKI D HACKBARTH G BULMASH AMSRL-WT-WD A NIILER AMSRL-WT-D D ECCLESHALL AMSRL-WT-T T WRIGHT AMSRL-MA-DA D DANDEKAR S CHOU R RAJENDRAN AMSRL-MA-C D VIECHNICKI M SLAVIN AMSRL-MA-CC M WELLS

No. of Copies	Organization
2	FRANHOFER-INSTITUT-FÜR-KURZZEITDYNAMIK ERNST-MACH-INSTITUT ATTN: H SENF E STRASSBURGER HAUPTSTRASSE 18 D-79 576 WEIL AM RHEIN GERMANY
3	FRANHOFER-INSTITUT-FÜR-KURZZEITDYNAMIK ERNST-MACH-INSTITUT ATTN: G SCHRÖDER A STILP V HOHLER ECKERSTRAßE 4 D-79 104 FREIBURG GERMANY
3	DEUTSCH-FRANZÖSISCHES FORSCHUNGSINSTITUT SAINT-LOUIS ATTN: H ERNST H LERR K HOOG CÉDEX 5, RUE DU GÉNÉRAL CASSAGNOU F-68301 SAINT LOUIS FRANCE
5	DEFENCE RESEARCH AGENCY ATTN: W CARSON T HAWKINS B SHRUBSALL C FREW I CROUCH CHOBHAM LANE CHERTEY SURREY KT16 OEE UNITED KINGDOM
1	DEFENCE RESEARCH AGENCY ATTN: T BARTON FT. HALSTEAD SEVEN OAKS KENT TN14 7BP UNITED KINGDOM
1	BATTELLE INGENIEURTECHNIK GMBH ATTN: W FUCHE DUESSELDORFLER STR. 9 D-65760 ESCHBORN GERMANY

No. of Copies	Organization
1	DEUTSCHE AEROSPACE AG ATTN: M HELD POSTFACH 13 40 D-86 523 SCHROBENHAUSEN GERMANY
2	RAPHAEL BALLISTICS CENTER ATTN: Y PARTOM G ROSENBERG BOX 2250 HAIFA 31021 ISRAEL
1	DYNAMEC RESEARCH AB ATTN: Å PERSSON PARADISGRÄND 7 S-151 36 SÖDERTÄLJE SWEDEN
1	DEFENCE RESEARCH ESTABLISHMENT SUFFIELD ATTN: C WEICKERT BOX 4000 MEDICINE HAT ALBERTA TIA 8K6 CANADA
1	DEFENCE RESEARCH ESTABLISHMENT-VALCARTIER ARMAMENTS DIVISION ATTN: RICHARD DELAGRAVE 2459 PIE X1 BLVD N P.O. BOX 8800 CORCELETTE, QUEBEC GOA 1RO CANADA
1	NATIONAL DEFENCE HEADQUARTERS ATTN: PMO-MRCV MAJ M PACEY NDHQ OTTOWA, ONTARIO KIA OK2 CANADA
1	EMBASSY OF AUSTRALIA ATTN: R WOODWARD COUNSELLOR DEFENCE SCIENCE 1601 MASSACHUSETTS AVE NW WASHINGTON, DC 20036-2273

No. of Copies	Organization
4	CENTRE DE RECHERCHES ET D'ETUDES D'ARCUEIL ATTN: F TARDIVAL C COTTENNOT S JONNEAUX H ORSINI 16 BIS AVENUE PRIEUR DE LA CÔTE D'OR F-94114 ARCUEIL CÉDEX FRANCE
1	INGENIEURBÜRO DEISENROTH ATTN: F DEISENROTH AUF DE HARDT 33-35 D-5204 LOHMAR 1 GERMANY
3	SWEDISH DEFENCE RESEARCH ESTABLISHMENT ATTN: B JANZON I MELLGARD L HOLMBERG BOX 551 S-147 25 TUMBA SWEDEN
1	TNO PRINS MAURITS LABORATORY ATTN: H PASMAN P.O. BOX 45 2280 AA RIJSWIJK LANGE KLEIWEG 137 RIJSWIJK, NETHERLANDS
2	DEFENCE TECHNOLOGY AND PROCUREMENT AGENCY ATTN: G LAUBE W ODERMATT BALLISTICS, WEAPONS AND COMBAT VEHICLE TEST CENTER CH-3602 THUN SWITZERLAND
1	SWISS FEDERAL ARMAMENT WORKS ATTN: W LANZ ALLMENDSSTRASSE 86 CH-3602 THUN SWITZERLAND

No. of Copies	Organization
1	NATIONAL DEFENCE RESEARCH ESTABLISHMENT DIVISION OF MATERIALS ATTN: SJ SAVAGE S-172 90 STOCKHOLM SWEDEN

USER EVALUATION SHEET/CHANGE OF ADDRESS

This Laboratory undertakes a continuing effort to improve the quality of the reports it publishes. Your comments/answers to the items/questions below will aid us in our efforts.

1. ARL Report Number/Author ARL-TR-1146 (Burkins) Date of Report July 1996

2. Date Report Received _____

3. Does this report satisfy a need? (Comment on purpose, related project, or other area of interest for which the report will be used.) _____

4. Specifically, how is the report being used? (Information source, design data, procedure, source of ideas, etc.) _____

5. Has the information in this report led to any quantitative savings as far as man-hours or dollars saved, operating costs avoided, or efficiencies achieved, etc? If so, please elaborate. _____

6. General Comments. What do you think should be changed to improve future reports? (Indicate changes to organization, technical content, format, etc.) _____

CURRENT ADDRESS

_____
Organization

_____
Name

_____
Street or P.O. Box No.

_____
City, State, Zip Code

7. If indicating a Change of Address or Address Correction, please provide the Current or Correct address above and the Old or Incorrect address below.

OLD ADDRESS

_____
Organization

_____
Name

_____
Street or P.O. Box No.

_____
City, State, Zip Code

(Remove this sheet, fold as indicated, tape closed, and mail.)
(DO NOT STAPLE)